BRAIN CONNECTIVITY
Volume 13, Number 7, 2023

DOI: 10.1089/brain.2022.0074

Efficiency of Heterogenous Functional Connectomes Explains Variance in Callous-Unemotional Traits After Computational Lesioning of Cortical Midline and Salience Regions

Drew E. Winters,[1] Daniel R. Leopold,[1] Joseph T. Sakai,[1] and R. McKell Carter[2–4]

Abstract

Introduction: Callous-unemotional (CU) traits are a youth antisocial phenotype hypothesized to be a result of differences in the integration of multiple brain systems. However, mechanistic insights into these brain systems are a continued challenge. Where prior work describes activation and connectivity, new mechanistic insights into the brain's functional connectome can be derived by removing nodes and quantifying changes in network properties (hereafter referred to as computational lesioning) to characterize connectome resilience and vulnerability.
Methods: Here, we study the resilience of connectome integration in CU traits by estimating changes in efficiency after computationally lesioning individual-level connectomes. From resting-state data of 86 participants (48% female, age 14.52 ± 1.31) drawn from the Nathan Kline institute's Rockland study, individual-level connectomes were estimated using graphical lasso. Computational lesioning was conducted both sequentially and by targeting global and local hubs. Elastic net regression was applied to determine how these changes explained variance in CU traits. Follow-up analyses characterized modeled node hubs, examined moderation, determined impact of targeting, and decoded the brain mask by comparing regions to meta-analytic maps.
Results: Elastic net regression revealed that computational lesioning of 23 nodes, network modularity, and Tanner stage explained variance in CU traits. Hub assignment of selected hubs differed at higher CU traits. No evidence for moderation between simulated lesioning and CU traits was found. Targeting global hubs increased efficiency and targeting local hubs had no effect at higher CU traits. Identified brain mask meta-analytically associated with more emotion and cognitive terms. Although reliable patterns were found across participants, adolescent brains were heterogeneous even for those with a similar CU traits score.
Conclusion: Adolescent brain response to simulated lesioning revealed a pattern of connectome resiliency and vulnerability that explains variance in CU traits, which can aid prediction of youth at greater risk for higher CU traits.

Keywords: adolescents; brain heterogeneity; callous-unemotional traits; computational lesioning; functional connectivity; topology

Impact Statement

Mechanistic insights into the differences in multiple brain systems underlying callous-unemotional (CU) traits represent a continued challenge. By examining changes in the brain functional connectome after computationally lesioning that node and examining changes in network properties, we can derive unique mechanistic insights. By applying this method to individual-level connectomes, we revealed a pattern of vulnerability and resiliency in the individual-level connectomes that aid the prediction of CU traits. Regions revealed with this method contextualize behavioral impairments in these youth, and this mask of identified regions could improve the prediction of youth higher in CU traits.

[1]Department of Psychiatry, University of Colorado School of Medicine Anschutz Medical Campus, Aurora, Colorado, USA.
[2]Department of Psychology & Neuroscience; [3]Institute of Cognitive Science; [4]Department of Electrical, Computer and Energy Engineering; University of Colorado Boulder, Boulder, Colorado, USA.

Introduction

Callous-unemotional (CU) traits are an antisocial phenotype in youth related to the affective impairments in adult psychopathy (Barry et al., 2000; Frick and White, 2008; Frick et al., 2014a) and are defined by impairments in prosocial emotions such as remorse, guilt, and empathy (Frick et al., 2014a; Frick et al., 2014b). The CU traits are associated with persistent criminal behavior (Kahn et al., 2013) and higher substance use (Winters et al., 2021a) while causing substantial costs to society (Kiehl and Hoffman, 2011).

Available treatments, however, are limited in their efficacy, indicating the need to better understand the mechanisms underlying these traits (for review: White et al., 2022). Brain mechanisms underlying CU traits have been conceptualized as involving either under-activation of the modular regions involved in salience (Blair and Frith, 2000; Patrick, 1994) or less efficient integration between multiple brain networks (impaired integration theory; Hamilton et al., 2015).

But, extracting mechanisms from this work is an ongoing challenge, which is plausibly due to the following three reasons. First, rather than modular activation, to understand integration across multiple brain systems, we need to consider how different and potentially distant hubs respond to perturbations of a given network node (i.e., node removal) using computationally simulated lesions (Honey and Sporns, 2008). Second, the shape of brain networks and resulting information processing streams (i.e., topology) (De Vico Fallani et al., 2014; Kaiser et al., 2015) are rarely examined in studies on CU traits.

Finally, the substantial heterogeneity of individual connectomes (Damoiseaux et al., 2021) and their heterogeneous association with both psychopathy (Dotterer et al., 2020) and CU traits (Winters et al., 2021c) need to be accounted for to make accurate inferences (Gates and Molenaar, 2012; Molenaar, 2004). Thus, the present study examines the topological brain properties underlying CU traits by examining individual-level brain responses with computational lesioning to understand the functional architecture accounting for variance in CU traits and underlying etiology.

Etiological theories of CU traits posit primary impairments that center on either affective (Blair, 2008; Hawes and Dadds, 2012) or cognitive deficits (i.e., attention and cognitive control) (Hamilton and Newman, 2018), with both positions supported by neurobiological evidence. For example, affective processing deficits include salience regions such as the insula and amygdala (Seara-Cardoso et al., 2016), with the majority of studies focusing on the amygdala in psychopathy (Blair and Frith, 2000; Patrick, 1994) and CU traits (Marsh et al., 2008). Cognitive deficits involve social and control regions in cortical midline structures such as the medial/lateral prefrontal cortices and anterior/posterior cingulate.

Less activation of these regions is observed during top-down attention (Larson et al., 2013; Newman and Baskin-Sommers, 2012), reward anticipation (Veroude et al., 2016), and decision-making tasks involving conflict monitoring (Abe et al., 2018; White et al., 2013). Whether these cognitive results indicate a general attention impairment or a tendency to not process affective information in the present context is debated (Blair and Mitchell, 2009); however, the ability to monitor and bring attention to context for regulating goal-directed behaviors (i.e., cognitive control; Botvinick et al., 2001) is an important impairment associated with CU traits (Gluckman et al., 2016) and related to decrements in representing others' affective states (Winters and Sakai, 2021) that are associated with differences in these multiple brain systems (Winters et al., 2022).

Impaired integration across these multiple brain systems (e.g., control, social, salience) is believed to underlie CU trait impairments beyond modular activation (impaired integration hypothesis) (Hamilton et al., 2015). Studies supporting this demonstrate less integration within and between networks involving regions outlined earlier, including the default mode network (DMN), frontoparietal network (FPN), and salience network (SAL).

For example, where we would expect greater connectivity within networks among healthy brains, CU traits are associated with less connectivity within the DMN (Cohn et al., 2015; Umbach and Tottenham, 2021), FPN (Winters et al., 2021c), and SAL (Yoder et al., 2016). Functional integration of these networks is also associated with normative brain processes (e.g., DMN and cognitive empathy) (Winters et al., 2021b) that are perturbed among individuals with elevated CU traits.

Further, where we would expect an anticorrelation between task-positive and task-negative networks in typically developing brains (Uddin et al., 2009), higher CU traits are associated with a diminished anticorrelation between the DMN and SAL (Winters and Hyde, 2022), as well as between the DMN and FPN (Pu et al., 2017; Winters et al., 2021c), which has also been found in adult psychopathy (Dotterer et al., 2020). This pattern of less connectivity within and between these networks is theorized to underlie cognitive impairments that impact affective processing (Hamilton et al., 2015), possibly via difficulties with perspective taking and cognitive control (Winters et al., 2022b).

It is necessary to also highlight the lack of convergence of the brain literature on CU traits and psychopathy that appears to point to more general topological properties of the brain. For example, task-based findings demonstrate some overlap but broadly heterogenous activation patterns among similar tasks (Seara-Cardoso et al., 2022); some connectivity studies did not find aberrant connectivity in the DMN (Pu et al., 2017) or in the SAL and FPN (Umbach and Tottenham, 2021), whereas other studies reviewed earlier did.

One possibility is that the brains of those higher in CU traits may have a less modular structure. Modularity describes the structure of the brain network representing the strength of divisions into network modules, with more modularity indicating dense connections within the network and less connections between networks (Newman and Girvan, 2004). Less modular structure of the brain results in less efficiency (Tosh and McNally, 2015), which impacts behavior and cognitive functioning (Rypma and Prabhakaran, 2009).

Decreased modularity could manifest in different networks of the brain (e.g., less connectivity of the DMN or the SAL) that could plausibly represent different subgroups of CU trait phenotypes. For example, CU traits have multiple presentations underlying individual differences (Fanti et al., 2018; Fanti et al., 2013; Hadjicharalambous and Fanti, 2018; Sebastian et al., 2012) and it is plausible that differential decrements in modularity of the DMN compared with the SAL may underlie these different subgroups. These hypotheses

remain speculative, however, and substantial methodological improvements are needed in this area of study.

The following three methodological improvements can help improve the characterization of neural substrates of CU traits. First, computational lesioning has yet to be applied to understand underlying functional brain properties of youth with CU traits. Computational lesioning probes the resilience or vulnerability of a functional network related to specific nodes, thereby providing valuable insights into entry points for mechanistic understanding of a disorder (Deco and Kringelbach, 2014).

Although real lesions involve long-term brain reorganization that is not captured when simulating lesions, computational lesioning confirms far-reaching disruptions of functional architecture that are related to the modular structure of nodes (e.g., global vs. local hubs) that is found in real lesions (Gratton et al., 2012; Tao and Rapp, 2021). Specifically, characterizing the disruptions that these different hubs cause on the connectome after computational lesioning is important for understanding underlying brain function (Honey and Sporns, 2008).

Second, although rarely studied in CU trait investigations, considering topological properties of the brain such as efficiency, modularity, and hubs can characterize how information is transferred in the brain. For example, measuring *efficiency* captures how information is exchanged in a network assuming that shorter distances between nodes is more efficient (Achard and Bullmore, 2007; Latora and Marchiori, 2001; Rubinov and Sporns, 2010), *modularity* captures within module density (Newman and Girvan, 2004), and *hubs* that are global or local captures whether a node is more connected across the brain or within a module (Gratton et al., 2012; Tao and Rapp, 2021).

The few studies of CU traits examining topology have identified important differences (Dotterer et al., 2020; Jiang et al., 2021; Winters et al., 2021c) that go beyond the typical considerations of functional activation and connection strength.

Third, letting go of the incorrect assumption of homogeneity in brain analyses can improve our statical inferences on potential mechanisms. For example, most relevant work uses group averages across the brain to make inferences. This would suggest an assumption of strict homogeneity of individual brains (Gates, 2022), but it is well known that functional brain patterns are as unique as fingerprints (Damoiseaux et al., 2021); thus, the assumption of homogeneity is incorrect.

Accordingly, recent studies demonstrate substantial heterogeneity of the brain in relation to CU traits (Winters et al., 2021c) and psychopathy (Dotterer et al., 2020). These studies demonstrate some shared patterns despite this heterogeneity (known as weak homogeneity) (Gates, 2022), which appears to more accurately reflect how we should model the brain. Failing to account for this individual variability when examining patterns across individuals leads to inaccurate inferences (Gates and Molenaar, 2012; Molenaar, 2004).

Thus, examining connectome efficiency across individual-level connectives using computational lesioning can improve our mechanistic understanding of CU traits by probing the resilience and vulnerability of an individual's functional connectome.

The way nodes in the functional connectome are connected can have different impacts on efficiency after computational lesioning. For example, a node can be globally connected, meaning it has denser connections across the brain between network modules, or can be locally connected, meaning it has denser connections within its respective network module and less connections with other modules—these are called global and local hubs, respectively (Gratton et al., 2012; Tao and Rapp, 2021).

Computational lesioning of global hubs reduces the number of long-range connections, resulting in more segregation of network modules, whereas lesioning of local hubs reduces the number of short-range connections, resulting in less segregation of network modules (Gratton et al., 2012; Sporns et al., 2007; Tao and Rapp, 2021). These forms of reorganization of the brain's modularity can have substantial impact on the brain's efficiency (Tosh and McNally, 2015).

Efficiency in the brains of those with CU traits is lower than controls (Jiang et al., 2021), which may be related to the global or local hub-like qualities (i.e., ''hubness'') of a given node. Despite not yet having been investigated, to our knowledge, data on how the efficiency of a network changes related to the properties of a node being a global or local hub could provide practical, functionally important mechanistic insights (Deco and Kringelbach, 2014). Thus, an important next step for understanding mechanisms underlying CU traits is to examine changes in efficiency using computational lesioning, characterize nodal ''hubness,'' and examine targeted lesioning of node types in relation to CU traits.

The present study examines the changes in efficiency after computationally simulating lesions in relation to CU traits among a community sample of adolescents. The CU traits exist along a continuum in community samples with substantial evidence of similar neurocognitive and neurobiological impairments as forensic samples with these traits (Seara-Cardoso et al., 2022; Viding and McCrory, 2012). In this sample of community adolescents, we hypothesize that the changes in efficiency after computationally simulating lesions can explain variance in and help us understand the mechanisms underlying CU traits.

Specifically, we hypothesize that the changes in response to cortical midline structures as well as regions associated with salience (amygdala and insula) will account for variance in CU traits. Consistent with the literature on global and local hub lesioning discussed earlier, we specifically anticipate that lesioning local hubs will demonstrate the greatest decrement in efficiency. In addition, in accordance with prior studies, we expect that modularity will account for variance in CU traits such that lower modularity will be associated with higher CU traits. This information has the potential to provide unique mechanistic insights that complement task-based and functional connectivity studies by identifying points of resilience and vulnerability in functional connectomes in relation to CU traits.

Methods

Sample

Participants were drawn from the Rockland study collected by the Nathan Kline Institute. We downloaded raw fMRI files and study measurements from the 1000

connectomes project. We included adolescent participants between the ages of 13 and 17 with an IQ >80 as measured by the WAIS-II ($\alpha = 0.96$) (Wechsler, 2011). We excluded potential participants with motion >3 mm or >20% of invalid functional magnetic resonance imaging (fMRI) scans.

Two participants had spikes in motion that were near the end of the session and were able to retain those participants by cutting their time series, leaving a total analysis sample of 86. The participants in this sample were predominantly White (White = 63%, Black = 24%, Asian = 9%, Indian = 1%, other = 3%), with 14% reporting Latinx ethnicity, mean age of 14.5 (14.52 ± 1.31) years, slightly more males (females = 48%), and mean pubertal development just below full maturity (4.10 ± 0.97; range 1–5). Nooner et al. (2012) outline study procedures, including consent and assent for all participants.

Measures

Inventory of callous-unemotional traits. The CU traits were assessed using the total score of the 24-item inventory of callous-unemotional traits (ICU) (Frick, 2004). Consistent with Kimonis et al. (2008), we removed two items with poor psychometrics, which had adequate reliability in the current sample ($\alpha = 0.72$). Higher scores indicate greater CU traits. The total ICU score was used as the primary outcome of interest.

Tanner stage. Sex and pubertal stage were measured using the Tanner assessment ($\alpha = 0.77$). Parents rated pictures of secondary sex characteristics, indicating pubertal development of 1 (pre-pubertal) to 5 (full maturity) (Petersen et al., 1988).

fMRI acquisition

Resting-state fMRI images from the Rockland dataset were collected by the Nathan Kline Institute using a Siemens TimTrio 3T scanner with a blood oxygen level dependent contrast and an interleaved multiband echo planar imaging (EPI) sequence. Each scan involved resting state (260 EPI volumes; repetition time [TR] = 1400 ms; echo time = 30 ms; flip angle = 65°; 64 slices, field of view (FOV) = 224 mm, voxel size = 2 mm isotropic, duration = 10 min) and a magnetization prepared rapid gradient echo (MPRAGE) anatomical image (TR = 1900 ms, flip angle = 9°, 176 slices, FOV = 250 mm, voxel size = 1 mm isotropic).

The Siemens sequence does not collect images until T1 stabilization is achieved, so removing scans was not necessary. Instructions for participants were to keep their eyes closed without falling asleep and to not think of anything while they let their mind wander.

Resting-state fMRI preprocessing

Imaging data were preprocessed with the standard preprocessing in the CONN toolbox (version 18b) (Whitfield-Gabrieli and Nieto-Castanon, 2012) that uses Statistical Parametric Mapping (SPM version 12) (Penny et al., 2011). Motion outliers were flagged for correction if >0.5 mm using the Artifact Detection Tools and regressed out using spike regression. Slice timing correction was not used given the fast multiband acquisition (Glasser et al., 2013; Wu et al., 2011).

The anatomic component-based noise correction method (aCompCor) (Whitfield-Gabrieli and Nieto-Castanon, 2012) was used to regress out cerebrospinal fluid and white matter noise. MPRAGE and EPI images were co-registered and normalized to an MNI template; and data were bandpass filtered between 0.008 and 0.09 Hz to retain resting-state signals. Finally, we parcellated these data into 164 ROIs using the Harvard Oxford atlas for cortical and sub-cortical areas (Desikan et al., 2006) as well as the Automated Anatomical Labeling Atlas for cerebellar areas (Tzourio-Mazoyer et al., 2002).

The use of both parcellations is the default parcellation used in the CONN toolbox, as the cerebellar areas from the Automated Anatomical Labeling atlas do not overlap with the cortical or sub-cortical nodes of the Harvard Oxford atlas.

We found that 24 participants had excess motion >3 mm and 4 had >20% of invalid scans. However, we were able to retain two of the participants with excess motion because this motion was at the end of the timeseries and was able to be snipped while still retaining >90% of the timeseries. This left a total of 86 participants for analysis.

Construction of individual-level functional connectomes

Single-subject connectomes were derived within python (version 3.9.5; Van Rossum and Drake, 2009) using the graphical lasso covariance estimator in the package ''scikit-learn'' (Pedregosa et al., 2011). This resulted in a brain-wide sparse precision matrix for each participant (sparsity proportion = 0.895 ± 0.005) that retained about 10.5% of connections across all participants.

As opposed to imposing arbitrary covariance thresholds that reflect unique characteristics of the sample, this sparse matrix approach was chosen because it uses a principled approach that retains meaningful connections after conditioning on the rest of the matrix (Smith et al., 2011; Varoquaux et al., 2010). The most connected regions included bilateral frontal pole and bilateral insular cortex, whereas the most disconnected regions were posterior and anterior cerebellar as well as the bilateral posterior temporal gyrus (Supplementary Table S1).

Individual-level brain connectivity measures

Functional brain properties were derived from network estimations using the python-based brain connectivity toolbox (Rubinov and Sporns, 2010). First, we applied the robust Louvain algorithm (Blondel et al., 2008; Lancichinetti and Fortunato, 2009) combined with an iterated fine-tuning algorithm to optimize identifying modular structures at the single-subject level (Sun et al., 2009) and address the Louvain algorithm's stochastic nature (Bassett et al., 2011).

Specifically, we estimated five communities for each participant to determine the optimal individual-level gamma parameter, re-estimated communities using the individual-level optimal gamma, calculated the similarity for each iteration for each participant, and then derived a single consensus community across all iterations at the single-subject level.

Using the tuned parameters described earlier, we calculated individual-level modularity, participation coefficient, and within-module degree z-score. The participation coefficient was used to identify global hubs, because it represents the

strength of cross-module connections; conversely, the within-module z-score was used to identify local hubs, because it measures the extent of intra-modular connections of each node (Guimera and Nunes Amaral, 2005).

To identify the hubness of each node, we used criteria by Tao and Rapp (2021) but, where they used mean and standard deviation, we used median and median absolute deviation (MAD) because it is not as subject to sampling effects (Leys et al., 2013). We used this to identify individual-level global hubs (participation coefficient >1 MAD+median) and local hubs (within-module degree z-score coefficient >1 MAD+median).

Consistent with prior computational lesion studies (He et al., 2009), we identified non-hubs that were connector (i.e., more likely to be connected across network) or periphery nodes (i.e., more connected within module) but did not meet hub criteria. Finally, we calculated individual baseline efficiency to compare the changes in efficiency after computational lesioning.

Computationally simulated lesions at the individual-level

To investigate the dynamics and probe resilience or vulnerability underlying individual-level connectomes, we applied a procedure to computationally simulate lesions (deletion) over the functional connectome (He et al., 2009). Specifically, we used node deletion across each participant's functional connectome with two separate approaches. The first was a sequential deletion procedure for each node across the brain, and the second targeted nodes with properties of global and local hubs separately and connector and periphery non-hubs separately.

After each computationally simulated lesion, we calculated brain efficiency and subtracted each participant's baseline efficiency score to assess the brain's response. In other words, we calculated the baseline efficiency for each participant, then recalculated efficiency after each simulated lesion, and finally subtracted the baseline efficiency score from the new efficiency score to measure the change in efficiency. This procedure of change after a simulated lesioning was adopted form prior work (Gratton et al., 2012; Tao and Rapp, 2021).

Feature selection

We conducted feature selection to reduce noise by retaining only those features that are the most pertinent and improve model performance (Dosenbach et al., 2010). Feature selection is the method of reducing the number of features used in the elastic net regression by retaining the most relevant features while removing the features that increase noise in the data. Specifically, we used the k-best feature selection using the f regression function within ''scikit-learn'' (Pedregosa et al., 2011) and conducted hyperparameter tuning of the number of k features selected to improve model performance.

This feature selection resulted in 26 features in the feature vector consisting of: 23 nodes (23 features) representing changes in efficiency for each participant's functional connectome after removing that node, overall brain modularity (24th feature), and Tanner stage (25th feature). We also included sex (26th feature) independently of feature selection because of its implications for differences in the brain and CU traits in youth (Raschle et al., 2018). Importantly, head motion was not selected as accounting for substantial variance; thus, it was not included in the model. Brain features were placed in the model as independent variables to decode what brain activity predicts CU traits.

Elastic net regression

A linear elastic net regression was implemented in the python package ''scikit-learn'' (Varoquaux et al., 2010) to evaluate the relationship between functional connectome change in efficiency after removing each node. This is the primary analysis testing what features account for variance in CU traits. Model performance was evaluated using a nested five-fold cross-validation procedure involving hyper-parameter tuning and cross-validation.

What this means is that we conducted fivefold cross-validation but within each fold hyperparameters for the elastic net (i.e., L1 and L2 penalties) were tuned to ensure each fold had optimal hyperparameters. We used mean squared error, R^2, and mean absolute error to evaluate the model as well as comparing training and testing cross-validation scores. In addition, we compared the model with a dummy model to assess whether the model performed better than chance using the mean squared error.

We then assessed cumulative empirical distribution of model performance under the null hypothesis using a permutation test with 2000 iterations. Results were considered statistically significant if 95% of these 2000 R^2 values were lower than the R^2 of the real data (Dosenbach et al., 2010).

Meta-analytic decoding

For connection response to brain regions accounting for variation in CU traits, we used Neurosynth to meta-analytically annotate their functional characteristics. The automated neuroimaging meta-analysis computed whole-brain posterior activation distributions $P(Term \mid Activation)$ for the psychological concepts examined (Yarkoni et al., 2011). Terms that have been consistently associated with a particular activation map can be identified using unbiased reverse-inference analyses across the Neurosynth database.

At the time of writing this article, Neurosynth database contained maps for 1334 terms, 507,891 coordinates extracted from 14,371 fMRI studies, and coactivation maps for 150,000 brain locations. Using this database, we first decoded the mask of regions in our analysis, and second, we identified regional terms loading on to CU traits and psychopathy.

First, to decode the mask of identified ROIs during feature selection, we took the coordinates of all 23 regions and created a mask with 8 mm spheres around the center of each coordinate using the python package ''nltools'' (Chang, 2020) that is publicly available. This mask was used to then characterize co-activation of brain regions across studies in the Neurosynth database.

Statistical inference for each voxel in the brain volume was conducted using chi-square tests to generate a z-value map thresholded with a false discover-rate adjusted p-value of $p < 0.01$; and the voxel-wise correlation coefficient between the co-activation map and each term-specific map was assessed for extraction. To obtain a large enough number to account for variation, the top 40 terms (e.g., executive

functioning, affect response; excluding methodological techniques [e.g., fMRI] or anatomy terms [e.g., prefrontal cortex]) were taken as the most likely associated terms. We assessed ambiguous terms by examining the top 10 loading studies to determine inclusion or exclusion.

For example, the term ''amygdala response'' involved the study of response to emotional stimuli; thus, it was included given that it is the brain's response to emotional stimuli. We averaged *R* values for terms that have common root terms (e.g., feeling and feelings). In addition, we placed each term in a general category (e.g., emotion, cognitive) that represents the studies under that term.

Second, we examined the identified region terms and extracted loading values on CU traits and psychopathy. We choose CU traits and psychopathy as our primary terms, because CU traits represent the affective dimension of psychopathy (Barry et al., 2000; Frick et al., 2014a) and brain features are shared between psychopathic adults and youth with CU traits (Seara-Cardoso et al., 2022). We searched variations of terms for CU traits (callous-unemotional, callous, callousness) and psychopathy (psychopathic, psychopath), reviewed the highest loading studies to ensure construct consistency, and extracted the loading value for that brain area and term.

Random-effects models, node characterization, and evaluating moderation

To contextualize brain properties related to the model results, linear random-effects models were conducted in python (version 3.9.5) (Van Rossum and Drake, 2009) using the ''statsmodels'' package (Seabold and Perktold, 2010) to characterize selected nodes, test for mediation, and test the impact of targeting global and local nodes. For all models, we accounted for random intercept variation for each participant. Confidence intervals for each parameter were bootstrapped with 2000 resamples.

We conducted secondary analysis that characterized nodes included in the elastic net model by evaluating whether their global or local ''hubness'' was associated with CU traits using separate regressions. Importantly, nine nodes were excluded from analyses characterizing global hubs because zero participants had a global hub for that node. To assess whether nodes' global or local ''hubness'' was different at higher CU traits from what was typically expected, we compared the probability of being a global or local hub for each node against a random distribution to assess whether the current sample's probability was better than chance.

We evaluated sex, modularity, and Tanner stage as potential moderators of above brain associations because both sex (Raschle et al., 2018) and pubertal stage (Cameron, 2004; Dahl, 2004; Sisk and Foster, 2004) demonstrate important differences in brain development and CU traits, and modularity can influence efficiency. First, we identified which of the above to evaluate based on significance in relation to CU traits in the elastic net model.

We then ran correlations of the significant independent variables with every significant node in the elastic net regression and identified which nodes they may be a moderator for by selecting correlation values that were 2 MAD greater or less the median *R* value. Potential moderation terms were derived using the residualized centering approach using the python package ''resmod'' (Winters, 2022). This approach orthogonalizes included terms by centering the residuals, thereby avoiding the violation of model assumptions by removing correlated residuals (Little et al., 2006). Confidence intervals were bootstrapped with 2000 resamples to test moderation.

Results

Lesioning nodes negatively impacted efficiency across all participants

Changes in efficiency after node deletion were, on average, negative for all nodes across the sample. The magnitude of this decrement varied by node (Table 1). Thus, positive associations in the following analyses represent the connectomes resilience because the change is closer to zero and negative associations represent a greater decrement in efficiency.

Computational lesioning of brain nodes predicts CU traits

Feature selection identified 23 brain nodes, modularity, and Tanner stage as features that improved the prediction of CU traits (see Table 1 for coordinates of brain features and Fig. 1C for all features). The elastic net model performed better than a dummy model and we found no evidence of overfitting (Table 2). As shown in Figure 1A, the association between predicted score and observed score for CU traits was significant ($R^2 = 0.311$, $p_{perm} < 0.001$).

The observed R^2 in the permutation distribution is plotted in Figure 1B. Figure 1C plots the distribution of cross-validation betas for each feature in the model. These results suggest that the elastic net model performed satisfactorily in predicting CU traits.

Ten features are negatively associated with CU traits: modularity, aMTG L, toITG L, SPL L, ICC L, PT R, Ver 3 and 9, anterior insula R, and SMG L (all abbreviations are in Table 1). Modularity indicates that those with higher CU traits tended to have a less modular structure. The brain nodes indicate that a greater decrement in efficiency after computationally lesioning that node is associated with higher CU traits. Fourteen features are positively correlated with CU traits: Tanner stage, IFG oper L, TP L, PostCG L, SMA L, AC, Cuneal L, aTFusC L, pTFusC R, FO L, PO L, Amygdala L, PCC, and IFG R (all abbreviations are in Table 1).

Tanner stage indicates that those further along in pubertal development demonstrate higher CU traits. The remaining nodes indicate that less of a change in efficiency after lesioning each node is associated with more CU traits. The two features that could not be distinguished from zero were sex and the anterior cerebellar region. The full model weights for the features in the elastic net model and their corresponding R^2 and *p*-values derived from permutations are provided in Table 3, and the brain region beta weights are depicted in Figure 2.

Meta-analytic decoding of region mask identified emotional terms

The mask of regions used in the elastic net model is associated with several maps within Neurosynth covering emotions and affective information processing (Fig. 3). The five terms with the highest associations involved the amygdala's response to affective stimuli, mood, neutral (emotions), semantic control, and emotion regulation. When

Table 1. Selected Regions Coordinates, Abbreviations Used, and Descriptives on Change in Efficiency

Area	Abbreviation	Coordinate			Efficiency change	
		X	*Y*	*Z*	*Mean*	*SD*
Cerebellar anterior	Cebellar.Anterior	0	−63	−30	−0.0067	0.0004
Inferior frontal gyrus R	Language.IFG R	54	28	1	−0.0065	0.0004
Supramarginal gyrus L	Salience.SMG L	−60	−39	31	−0.0067	0.0005
Anterior insula R	Salience.Ainsula R	47	14	0	−0.0067	0.0004
Posterior cingulate cortex	DefalutMode.PCC	1	−61	38	−0.0069	0.0005
Vermis 9	Ver9	1	−55	−35	−0.0066	0.0005
Vermis 3	Ver3	1	−40	−11	−0.0063	0.0004
Amygdala L	Amygdala L	−23	−5	−18	−0.0064	0.0004
Planum temporale R	PT R	55	−25	12	−0.0067	0.0004
Parietal operculum L	PO L	−48	−32	20	−0.0065	0.0003
Frontal pole L	FP L	−40	18	5	−0.0060	0.0004
Temporal fusiform cortex posterior division R	pTFusC R	36	−24	−28	−0.0067	0.0004
Temporal fusiform cortex anterior division L	aTFusC L	−32	−4	−42	−0.0067	0.0004
Cuneal L	Cuneal L	−8	−80	27	−0.0066	0.0004
Anterior cingulate	AC	1	18	24	−0.0067	0.0004
Supplementary motor area L	SMA L	−5	−3	56	−0.0066	0.0004
Intracalcarine cortex L	ICC L	−10	−75	8	−0.0064	0.0004
Superior parietal lobule L	SPL L	−29	−49	57	−0.0068	0.0004
Postcentral gyrus L	PostCG L	−38	−28	52	−0.0067	0.0004
Inferior temporal gyrus temporooccipital L	toITG L	−52	−53	−17	−0.0069	0.0004
Middle temporal gyrus anterior division L	aMTG L	−57	−4	−22	−0.0069	0.0006
Temporal pole L	TP L	−40	11	−30	−0.0050	0.0008
Inferior frontal gyrus pars opercularis L	IFG oper L	−51	15	15	−0.0069	0.0005

Efficiency change is the change in baseline efficiency after lesioning the brain region.
SD, standard deviation.

placed in the respective categories, emotional terms were of the most prominent category with 29 terms followed by 9 cognitive terms and 2 related to disorders (post traumatic stress disorder and anxiety disorder).

Meta-analysis of node terms loaded on CU traits and psychopathy

A total of 13 nodes loaded on to CU traits and/or psychopathy, with the amygdala having the highest loading value. Three of the nodes loaded on to CU traits, and all 13 loaded on to psychopathy. A total of 10 nodes associated with adult psychopathy but had not yet been identified in youth with CU traits among the studies within Neurosynth.

Node hub differences at higher CU traits

There were only a few nodes for which hubness associated with CU traits, but these hubs were notably less likely to be a hub (either global or local) over the entire sample. For global hubs, only the IFG oper L being a global hub associated with higher CU traits (Std $\beta = 0.178$, $p = 0.006$). Importantly, across the entire sample the probability of that region being considered a hub was only 4.7% (Table 4) and was not better than chance at being a global hub.

For local hubs, the aMTG L (Std $\beta = 0.304$, $p = 0.002$), SPL L (Std $\beta = 0.287$, $p < 0.001$), ICC L (Std $\beta = 0.054$, $p = 0.025$), Cuneal L (Std $\beta = 0.110$, $p = 0.022$), and IFG R (Std $\beta = 0.078$, $p = 0.038$) being a local hub associated with higher CU traits. Again, the probability of these regions being a local hub across the sample was low (<17%) and not better than chance (Table 5). Common node hubs across the sample were identified for global hubs (AC, FO L, Amygdala L, and IFG R; Table 4) as well as local hubs (none; Table 5).

Targeting global hubs had less impact, whereas connector non-hubs decreased efficiency

Less change in efficiency after computationally lesioning global hubs was positively associated with higher CU traits (Std $\beta = 0.210$, $p = 0.006$), but targeting local hubs did not produce significant effects (Table 6). A greater decrement in efficiency after lesioning connector non-hubs was also associated with higher CU traits (Std $\beta = -0.184$, $p = 0.024$), but targeting peripheral nodes was not statistically significant (Table 7).

No evidence of moderation

We found no statistically meaningful moderations for modularity or Tanner stage. Results of these analysis are placed in Supplementary Tables S2 and S3.

Heterogenous functional connectomes evidence weak homogeneity

Figure 4 depicts the heterogeneity of individual brains even among those with higher or lower CU traits. Results were able to evidence some pattern-level similarities at higher CU traits, but there was considerable heterogeneity at the individual level.

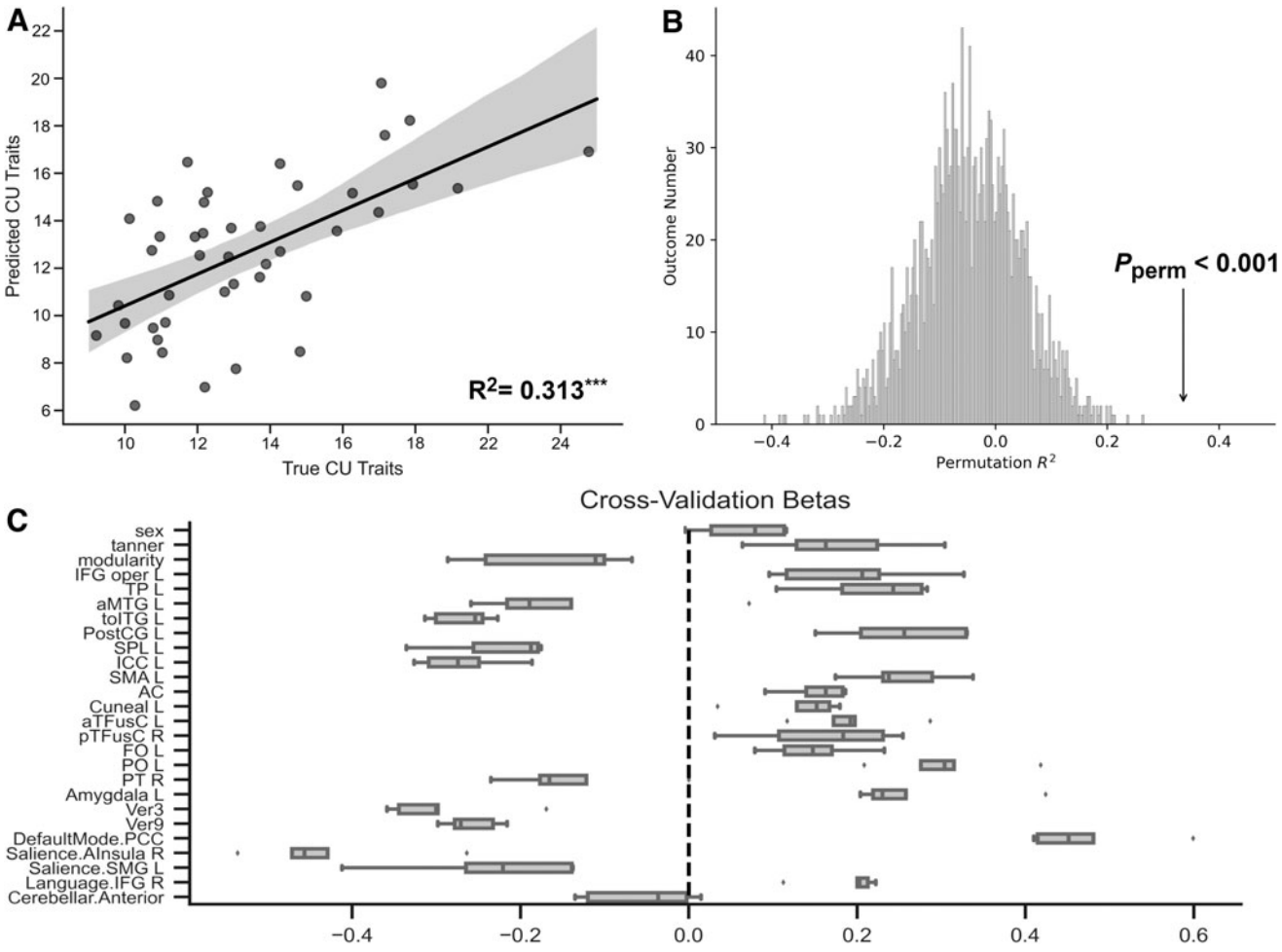

FIG. 1. Predicting continuous CU traits with elastic net regression using 26 selected features. **(A)** Regression line and true R^2 value. **(B)** Two thousand permutations testing of R^2 values for the model and permuted p-value for true R^2 value. **(C)** Fivefold cross-validation betas for each feature in the elastic net model that accounted for variance in CU traits. CU, callous-unemotional.

TABLE 2. ELASTIC NET CROSS-VALIDATION FIT STATISTICS

	Mean squared error		
Cross validation	*Elastic net*	*Dummy*	*Best fit*
Comparison to a dummy model			
1	7.522	10.265	Elastic net
2	4.168	5.946	Elastic net
3	9.042	21.315	Elastic net
4	5.875	7.941	Elastic net
5	7.651	9.588	Elastic net
	MSE	R^2	*MAE*
Elastic net model fit			
Training model	4.244 ± 0.268	0.601 ± 0.075	1.569 ± 0.060
Test model	6.784 ± 1.613	0.310 ± 0.123	2.00 ± 0.169
	True R^2	*Distribution*	p
Permutation R^2	0.313	0.146 ± 0.0922	<0.001

MAE, mean average error; MSE, mean standard error.

TABLE 3. BETA WEIGHTS AND PERMUTED *P* VALUES SORTED BY PERMUTED R^2

	Weights	R^2_{perm}	p_{perm}
DefaultMode.PCC	0.688*	0.077	0.033
Salience.Ainsula R	−0.496*	0.070	0.015
PO L	0.312*	0.049	0.001
Ver3	−0.227*	0.036	0.006
Amygdala L	0.198*	0.036	0.005
ICC L	−0.346*	0.033	0.016
PostCG L	0.285*	0.031	0.018
Modularity	−0.170*	0.024	0.006
Ver9	−0.135*	0.021	0.007
SPL L	−0.314*	0.021	0.037
Salience.SMG L	−0.191*	0.019	0.010
IFG oper L	0.094*	0.017	0.003
TP L	0.318*	0.017	0.028
FO L	0.214*	0.014	0.020
SMA L	0.453	0.012	0.056
pTFusC R	0.151*	0.012	0.003
AC	0.259*	0.008	0.028
Tanner	0.229*	0.006	0.034
toITG L	−0.434*	0.005	0.047
aMTG L	−0.024*	0.003	<0.001
Cerebellar.Anterior	−0.049	0.002	0.050
Language.IFG R	0.011*	0.001	<0.001
aTFusC L	0.003*	0.001	<0.001
Sex	0.040	0.001	0.060
PT R	−0.344	0	0.062
Cuneal L	0.002*	0	<0.001

*$p_{perp} < 0.05$.
R^2 and *p*-values tested with 2000 permutations.

Discussion

Overall results reveal that understanding efficiency changes after computational lesioning individual-level connectomes accounts for variation in CU traits in a community sample of adolescents. Moreover, the network properties of these nodes are important for distinguishing their impact on the network. The results of this study demonstrate the importance of topological features of the brain for gaining a mechanistic understanding of traits that may aid the identification of individuals higher in CU traits.

Lesioning nodes negatively impacted efficiency across all participants

As expected, the average response of the functional connectome for all selected nodes resulted in a reduction in efficiency. This reflects the importance of each individual node for the function of the entire brain, and removing any node has an impact on the brain's efficiency. Although this is a descriptive statistic, it is important for interpreting the results. Specifically, positive associations indicate resilience of the connectome because changes in efficiency are closer to

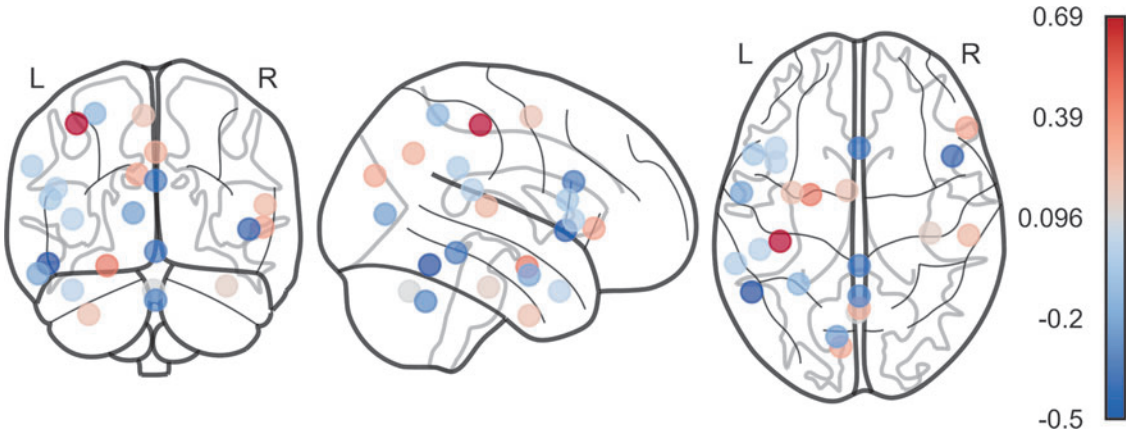

FIG. 2. Brain region mask and corresponding beta values accounting for variance in CU traits. Red and blue indicate positive and negative beta values, respectively. See Table 1 for coordinates of each region and Table 3 for specific beta values.

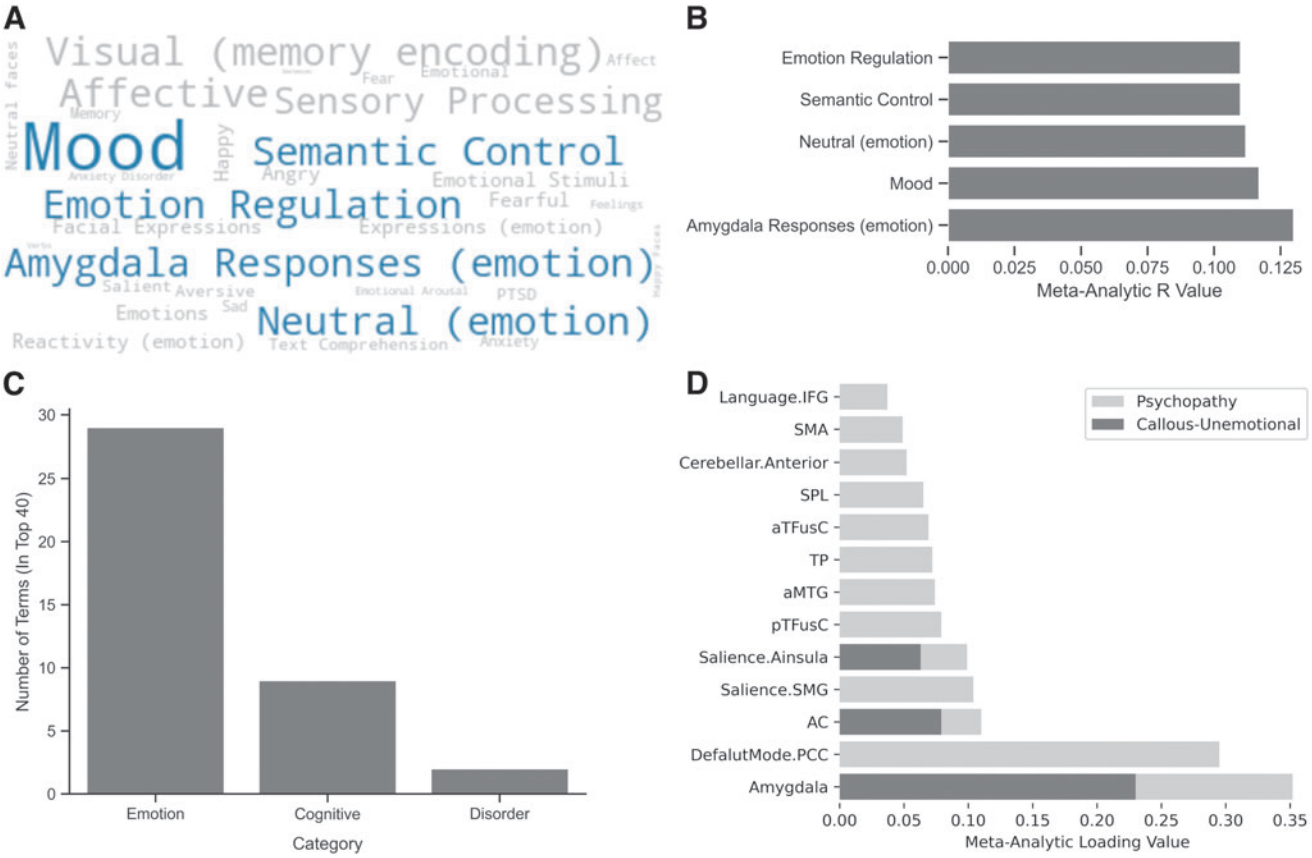

FIG. 3. Meta-analytic decoding demonstrating that emotional terms are associated with brain mask identified from simulated lesions and individual nodes loading on the CU traits and psychopathy. **(A)** Word cloud of top 40 terms where size indicates strength of correlation value and top 5 terms are outlined in light blue; **(B)** meta-analytic *R* values for the top 5 terms; **(C)** categories of identified terms; **(D)** loading of node terms on CU traits or psychopathy.

TABLE 4. RESULTS OF CHARACTERIZING *GLOBAL* NODES IN RELATION TO CALLOUS-UNEMOTIONAL TRAITS

						Bootstrapped, 95% CI		*Whole sample probability global hub*	
	Coef.	*Std.Coef*	*Std.Err.*	*z*	*p*	*Lower*	*Upper*	*Probability*	*>Chance*
IFG oper L	6.286*	0.178	2.275	2.763	0.006	1.827	10.746	0.047	False
PostCG L	1.617	0.139	1.104	1.464	0.143	−0.547	3.78	0.001	False
ICC L	0.428	−0.105	0.828	0.516	0.606	−1.195	2.051	0.001	False
SMA L	−0.005	−0.078	0.987	−0.005	0.996	−1.94	1.93	0.001	False
AC	1.179	0.017	0.887	1.329	0.184	−0.56	2.918	0.500	True
aTFusC L	1.237	0.015	1.056	1.171	0.242	−0.833	3.307	0.001	False
FO L	−0.215	−0.045	1.018	−0.211	0.833	−2.211	1.781	0.523	True
PO L	0.517	−0.064	0.989	0.523	0.601	−1.421	2.455	0.442	False
Amygdala L	1.564	−0.017	1.014	1.542	0.123	−0.424	3.552	0.547	True
Ver9	1.467	−0.002	0.951	1.542	0.123	−0.397	3.331	0.001	False
Salience.Ainsula R	0.280	0.136	1.152	0.243	0.808	−1.978	2.538	0.349	False
Salience.SMG L	0.543	−0.183	0.875	0.621	0.535	−1.172	2.259	0.001	False
Language.IFG R	−0.272	−0.159	0.918	−0.297	0.767	−2.071	1.527	0.512	True
Individual Var	8.925								

Nine nodes were excluded due to zero participants with a global hub for that node.

The whole sample probability test compares the whole sample probability of being a global node and compares this with a random sample. True indicates that the sample probability is better than chance, whereas False indicates that the sample probability is not better than chance.

See Table 1 for abbreviations for brain regions.

*$p < 0.05$.

CI, confidence interval.

Table 5. Results of Characterizing *Local* Nodes in Relation to Callous-Unemotional Traits

						Bootstrapped, 95% CI		*Whole sample probability local hub*	
	Coef.	*Std.Coef*	*Std.Err.*	*z*	*p*	*Lower*	*Upper*	*Probability*	*>Chance*
IFG oper L	1.790	0.069	1.138	1.573	0.116	−0.441	4.021	0.198	False
TP L	2.179	0.128	1.386	1.573	0.116	−0.537	4.895	0.140	False
aMTG L	3.851*	0.304	1.233	3.124	0.002	1.435	6.266	0.174	False
toITG L	−0.203	−0.155	1.16	−0.175	0.861	−2.476	2.07	0.186	False
PostCG L	0.295	−0.098	1.229	0.24	0.810	−2.113	2.704	0.151	False
SPL L	4.265*	0.287	1.193	3.574	<0.001	1.926	6.604	0.140	False
ICC L	2.822*	0.054	1.256	2.248	0.025	0.361	5.283	0.140	False
SMA L	1.549	0.034	1.285	1.206	0.228	−0.969	4.067	0.151	False
AC	1.663	−0.021	1.208	1.376	0.169	−0.705	4.03	0.151	False
Cuneal L	2.593*	0.110	1.132	2.29	0.022	0.373	4.812	0.174	False
aTFusC L	0.073	−0.173	1.151	0.063	0.95	−2.182	2.328	0.186	False
pTFusC R	0.243	−0.072	1.346	0.181	0.857	−2.395	2.881	0.174	False
FO L	0.253	−0.030	1.368	0.185	0.853	−2.429	2.934	0.163	False
PO L	0.065	−0.190	1.246	0.052	0.959	−2.379	2.508	0.221	False
PT R	2.074	0.069	1.303	1.592	0.111	−0.48	4.627	0.140	False
Amygdala L	1.055	−0.059	1.355	0.778	0.436	−1.601	3.710	0.151	False
Ver3	1.201	−0.001	1.112	1.079	0.28	−0.979	3.381	0.174	False
Ver9	−0.388	−0.120	1.264	−0.307	0.759	−2.865	2.089	0.174	False
DefaultMode.PCC	2.496	0.138	1.237	2.018	0.044	0.071	4.921	0.186	False
Salience.Ainsula R	−0.382	−0.110	1.147	−0.333	0.739	−2.63	1.866	0.163	False
Salience.SMG L	−0.445	−0.108	1.606	−0.277	0.782	−3.592	2.703	0.128	False
Language.IFG R	2.761*	0.078	1.331	2.075	0.038	0.153	5.37	0.116	False
Cerebellar.Anterior	−0.227	−0.124	1.238	−0.183	0.855	−2.654	2.20	0.198	False
Individual Var	7.705								

Whole sample probability compares the whole sample probability of being a local node and compares this with a random sample. True indicates that the sample probability is better than chance, whereas False indicates that the sample probability is not better than chance.
See Table 1 for abbreviations for brain regions.
*$p < 0.05$.

zero whereas a negative association indicates a node where the functional connectome is vulnerable.

Computational lesioning of brain nodes predicts CU traits

As anticipated, feature selection identified cortical midline regions (e.g., anterior cingulate, posterior cingulate cortex) and regions associated with salience detection (right anterior insula, left supramarginal gyrus, and left anterior amygdala). What was less expected is that elastic net weights reveal important regions where the functional connectome is resilient where it was not expected to be. For example, the weight for the left amygdala was positive, suggesting that there was less of a change in efficiency after removing that node.

The amygdala is a central hub for processing emotions and is heavily involved in social interactions (Bickart et al., 2014); thus, we would expect greater decrements after its removal. However, the resilience of the connectome at higher CU traits after removing the amygdala suggests that there is less integration with the rest of the connectome. Although many task-based studies found a lack of activation in the right amygdala at higher CU traits (Dotterer et al., 2017; Jones et al., 2009; Viding et al., 2012), our study, consistent with others (Marsh et al., 2008; Yang et al., 2009), reveals

Table 6. Results of Targeted Lesions for Global and Local Nodes Predicting Callous-Unemotional Traits

						Bootstrapped, 95% CI	
	Coef.	*Std.Coef*	*Std.Err.*	*z*	*p*	*Lower*	*Upper*
Intercept	6.468*	0.000	1.173	5.514	<0.001	1.678	11.771
Δ Global nodes	20.641*	0.210	7.567	2.728	0.006	1.714	42.429
Δ Local nodes	30.113	0.140	17.183	1.753	0.08	−12.041	71.427
Modularity	−209.001*	−0.220	99.053	−2.11	0.035	−482.037	3.366
Tanner	0.812	0.237	0.355	2.285	0.022	0.062	1.509
Sex	0.078	0.012	0.715	−0.109	0.913	−1.752	1.560
Individual var	4.997						

Global and local hubs were included in one analysis because of their statistical independence but not with their non-hub counterparts because of multicollinearity.
*$p < 0.05$.

TABLE 7. RESULTS OF TARGETED LESIONS FOR CONNECTOR AND PERIPHERY NODES PREDICTING CALLOUS-UNEMOTIONAL TRAITS

						Bootstrapped, 95% CI	
	Coef.	*Std.Coef*	*Std.Err.*	*z*	*p*	*Lower*	*Upper*
Intercept	−4.424	−0.001	4.333	−1.021	0.307	−13.574	1.1781
Δ Connector nodes	−22.817*	−0.181	10.107	−2.258	0.024	−42.462	−6.223
Δ Periphery nodes	−17.117	−0.132	23.39	−0.732	0.464	−85.450	19.768
Modularity	−204.058*	−0.215	99.714	−2.046	0.041	−490.497	−18.660
Tanner	0.836*	0.245	0.354	2.361	0.018	0.139	1.599
Sex	0.216	−0.028	0.681	0.317	0.751	−1.926	1.258
Individual var	6.361						

Connector and periphery non-hubs were included in one analysis because of their statistical independence but not with their hub counterparts because of multicollinearity.

*$p < 0.05$.

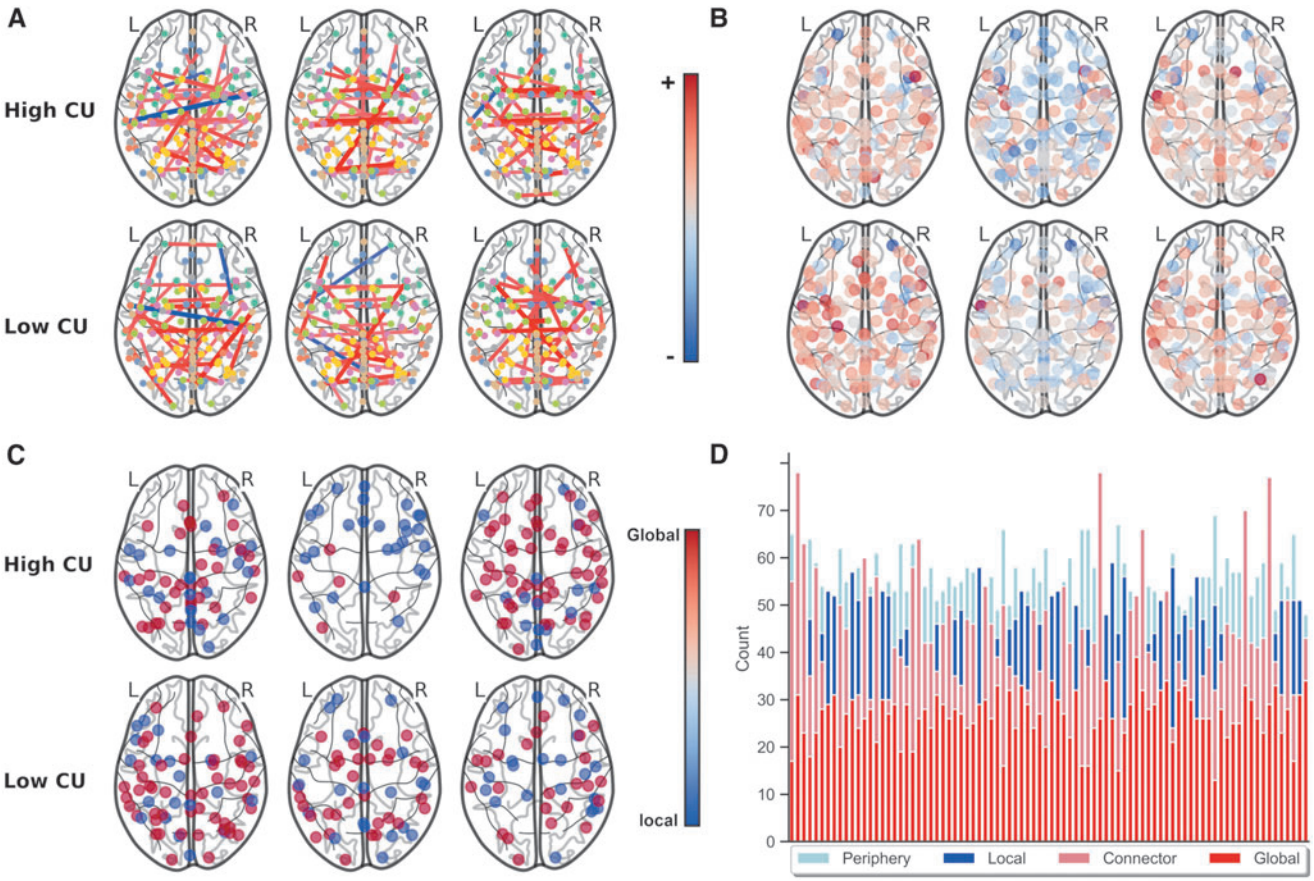

FIG. 4. Depicts the heterogeneity of adolescent brains even among those with similar scores at higher and lower CU traits. Meaning there are differences by individual even among those higher or lower in CU traits. Even though all analyses were done with continuous variables, we selected at random three participants with high and low levels of CU traits who were randomly selected to demonstrate heterogeneity within and between those at high and low CU traits. Note on color bars: the top color bar is for figures **(A, B)**, whereas the lower color bar is for figures **(C, D)**. **(A)** Individual-level functional connectomes demonstrate differences in connection (note some have negative connection and others do not and note the differences in positive connections); **(B)** changes in network efficiency after lesioning each node demonstrate differences in patterns of impact (note differences in the distribution of the positive and negative impact of lesioning each node); **(C)** location of global and local hubs demonstrates differences in hubness by individual (note different locations of global and local hubs); **(D)** number of hubs and non-hubs for each individual participant; each column is a participant, and it demonstrates different numbers of hubs.

that the left amygdala had less of an impact on the functional connectome's efficiency.

This discrepancy may be an artifact of stimuli presentation during a task-dependent state in prior studies (Funayama et al., 2001; Phelps et al., 2001). The present study did not impose a task-dependent state; thus, results plausibly reflect a more trait-like impairment involving less integration of the left amygdala associated with CU traits.

Additional positive associations were revealed in cortical midline structures, including the posterior cingulate and the anterior cingulate. The posterior cingulate is a central hub for information exchange (Leech et al., 2012) and is heavily involved in emotional arousal and attentional focus (Leech and Sharp, 2014) in healthy brains. The anterior cingulate is similarly involved in attention allocation, conflict monitoring, decision making, and emotion (Botvinick, 2007; Botvinick et al., 2004; Bush et al., 2000). As such, removal of these nodes was expected to impact the functional architecture of the brain in typically developing samples. However, less of a response of these nodes at higher CU traits suggests less integration with the rest of the connectome and less involvement in core processes for cognitive and emotional functioning.

However, lesioning other salience regions revealed a negative association of the right anterior insula and left supramarginal gyrus with CU traits. Where the right anterior insula is involved in attention (Eckert et al., 2009) involving interoceptive awareness (Craig, 2009, 2011) that aids both emotion and cognitive functioning (Touroutoglou et al., 2012), the left supramarginal gyrus is primarily involved in phonological processing (Celsis et al., 1999), though hypoactivity of this region has been associated with social cognition impairments in autism (Hadjikhani et al., 2006) and early psychosis (Park et al., 2021).

The negative impact on the functional connectome after removing these nodes may indicate an overreliance on these regions for similar processes that would be distributed across the amygdala and other cortical midline structures, leading to decreased whole-brain global efficiency. The differences in the brains' response to removal of these nodes characterize the impairments observed in CU traits as they appear to center around both cognitive and affective processing.

Modularity was another brain property accounting for variance in CU traits. Lower modularity, as revealed in prior work (Jiang et al., 2021), is associated with higher CU traits. Beyond differences in specific connections, decreased modularity may better describe the apparent lack of convergence among functional connectivity studies of CU traits, all of which generally demonstrate less intra-network connectivity and abnormal inter-network connections (Cohn et al., 2015; Umbach and Tottenham, 2021; Winters et al., 2021c; Yoder et al., 2016).

This is an important property that may lead to a better understanding of multiple CU trait variants underlying individual differences (Fanti et al., 2018; Fanti et al., 2013; Hadjicharalambous and Fanti, 2018; Sebastian et al., 2012). Specifically, which networks and the extent to which they exhibit decreased modularity may underlie differences in CU trait profiles.

Meta-analytic decoding of mask identified emotional terms

Meta-analytic decoding of the mask of regions identified in the present analysis primarily consisted of terms related to emotion and cognitive processes. Of the top 40 terms associated with the resulting mask, 29 were related to emotion processing (e.g., mood, amygdala response to emotion stimuli, and emotion regulation) and 9 involved cognitive processes (e.g., semantic control, cognitive encoding, and memory). This constellation of associations is consistent with the broader literature and theoretical accounts that CU traits involve both cognitive and, more substantially, affective processing impairments.

Meta-analysis of node terms loaded on CU traits and psychopathy

Meta-analytic activations in the identified nodes revealed 13 individual nodes loading on either CU traits or psychopathy. Of these nodes, the five highest loading nodes were the amygdala, posterior cingulate, anterior cingulate, left supramarginal gyrus, and anterior insula. Importantly, 10 of these nodes loaded only on psychopathy, which suggests that our results revealed brain regions associated with a related adult phenotype that was not previously found in CU traits. It is, therefore, plausible that this mask may provide a comprehensive picture of neural underpinnings that could help predict CU traits.

No evidence of moderation

There was no statistical evidence for modularity or Tanner stage moderating node efficiency changes related to CU traits. Moreover, the correlation between sex and CU traits did not meet study criteria to be further evaluated as a potential moderator. Overall, this suggests that the identified associations are direct and not affected by theoretically relevant, potential moderators.

Node hubness is different at higher CU traits

Both global and local hubs indicated at higher CU traits are not hubs in those that are lower in CU traits, suggesting a completely different topological structure at higher CU traits. Of the nodes surviving feature selection, a global hub in the IFG oper L and local hubs of the aMTG L, SPL L, ICC L, Cuneal L, and IFG R was associated with higher CU traits, which was different from the rest of the sample.

For example, the probability of the inferior frontal gyrus pars opercularis L being a global hub across the entire sample was about 4.7% and not better than chance even though its ''hubness'' was associated with elevated levels of CU traits. Similar results were also found among the aforementioned local hubs. Conversely, the amygdala has been demonstrated to be an important hub in the brain (Bickart et al., 2014) and the full sample results support this finding (i.e., the left amygdala was identified as a global hub above chance).

However, the left amygdala's likelihood of being a hub was not associated with CU traits. This specificity of CU-related hubs further highlights the notion that certain patterns of variation in brain topology likely account for differences in the brain's association with CU traits.

Targeting global hubs increased whereas connector non-hubs decreased efficiency

Targeting hubs and non-hubs revealed not only some similarities but also important differences in functional architecture

at higher CU traits. While targeting global hubs increased efficiency as expected, targeting local hubs had a positive trending yet non-significant effect despite predictions that doing so would decrease efficiency. Lesioning local hubs tends to remove shorter, more dense, and oftentimes more efficient connections, sparing longer and less efficient connections (Sporns et al., 2007; Tao and Rapp, 2021).

The fact that functional connectivity patterns of those higher in CU traits correlate with less modularity—and are therefore less likely to have highly interconnected sets of local connections aiding efficiency—may explain why there was less of an impact on connectomes when attacking these nodes at higher CU traits.

Efficiency changes after computationally lesioning connector non-hubs were negatively associated with CU traits. Because these nodes are more connected but do not possess the far-reaching connections of global hubs (He et al., 2009; Tao and Rapp, 2021), these nodes are more likely to have shorter, more abundant connections that are critical for efficient functional connectivity. Thus, this finding is consistent expectations that lesioning connector non-hubs would logically negatively impact efficiency.

Weak homogeneity of brains in relation to CU traits

While pattern-level similarities were identified in relation to CU traits, substantial heterogeneity exists between individuals' brains. This substantiates the weak homogeneity assumption (Gates, 2022) and, consistent with prior work (Dotterer et al., 2020; Winters et al., 2021c), stresses the need to account for individual heterogeneity of the brain's functional architecture in relation to CU traits. As such, we believe that our decision to not impose unrealistic homogeneity assumptions on adolescent brains lends itself to greater confidence in this study's results.

Limitations

The current study's results should be interpreted with the following limitations in mind. First, the present study had a modest sample size that may have missed some important effects. For example, sex effects were trending as expected, but we may not have had sufficient power to detect these effects. Knowing whether sex moderates the relationships observed is worthy of future study, and the identified brain mask should be applied to larger samples with adequate distributions of males and females.

Second, we sampled a range of ages that span multiple adolescent developmental stages (i.e., early to mid-adolescents), and larger samples within or across age bands would permit testing for age-specific differences. Third, while identified effects explained variance in CU traits, directionality cannot be determined from this cross-sectional sample. Longitudinal studies are needed to better examine the possibility of causality.

Finally, the sample analyzed was a community sample that, although exhibiting similar neurocognitive (Viding and McCrory, 2012) and neurobiological impairments (Seara-Cardoso et al., 2022) as forensic individuals, may not adequately capture the extremely high levels of CU traits seen among forensic and clinical samples. As such, sampling community along with clinical and forensic samples are needed for future investigations of this nature.

Conclusions

The present analyses demonstrate that knowing information about how individual-level brain connectomes respond to computationally simulated lesioning can explain meaningful variance in CU traits. This work identifies which nodes of adolescents' functional connectomes are more resilient or vulnerable to computational lesioning and how this pattern differs among individuals with high levels of CU traits. For example, the left amygdala is a central and highly connected node that aids the coordination of salience and emotion processing in typically developing samples; the lack of response observed in the current study, however, suggests that the brain's topological structure differs substantially at higher levels of CU traits.

Similar results implicate the anterior cingulate and posterior cingulate cortices, cortical midline structures that are pivotal for conflict monitoring, attention, and emotion processing. These differences plausibly account for behavior differences related to neurocognitive and emotional processes observed among youth with elevated CU traits. Further topological differences were observed when lesioning local hubs did not impact efficiency as expected.

These are important features describing qualities of information processing streams in the brain of youth with CU traits that suggest functional differences beyond activation or connection strength. Together, these results indicate a pattern of resilience and vulnerability, as well as underlying topological structure, characterizing CU traits. Future studies can advance our understanding of CU traits by using these identified regions to further investigate functional brain properties underlying CU traits as well as replication of predicting the severity of CU traits.

Acknowledgments

The authors acknowledge that an earlier version of this manuscript was published on a preprint server under the following citation: Winters DE, Leopold DR, and Sakai JT, et al. Efficiency of heterogenous functional connectomes explains variance in callous-unemotional traits after computational lesioning of cortical midline and salience regions. bioRxiv 2022–2010; doi: 10.1101/2022.10.07.511379.

Authors' Contributions

D.E.W.: conceptualization, methodology, software, formal analysis, data curation, writing—original draft, writing, review and editing, and visualization. D.R.L.: Writing—review and editing. J.T.S.: writing—review and editing, supervision, and resources. R.M.C.: writing—review and editing, supervision.

Author Disclosure Statement

No competing financial interests exist.

Funding Information

Drew E. Winters and Daniel R. Leopold were supported by a training grant from the National Institutes of Mental Health, T32MH015442. Joseph T. Sakai was supported by a grant from the National Institute of Drug Addiction, UG3DA054746.

Supplementary Material

Supplementary Table S1
Supplementary Table S2
Supplementary Table S3

References

Abe N, Greene JD, Kiehl KA. Reduced engagement of the anterior cingulate cortex in the dishonest decision-making of incarcerated psychopaths. Soc Cogn Affect Neurosci 2018; 13(8):797–807; doi: 10.1093/scan/nsy050

Achard S, Bullmore E. Efficiency and cost of economical brain functional networks. PLoS Comput Biol 2007;3(2):e17.

Barry CT, Frick PJ, DeShazo TM, et al. The importance of callous-unemotional traits for extending the concept of psychopathy to children. J Abnorm Psychol 2000;109(2):335–340; doi: 10.1037/0021-843x.109.2.335

Bassett DS, Wymbs NF, Porter MA, et al. Dynamic reconfiguration of human brain networks during learning. Proc Natl Acad Sci U S A 2011;108(18):7641–7646.

Bickart KC, Dickerson BC, Barrett LF. The amygdala as a hub in brain networks that support social life. Neuropsychologia 2014;63:235–248.

Blair RJ, Mitchell DG. Psychopathy, attention and emotion. Psychol Med 2009;39(4):543–555; doi: 10.1017/s0033291708003991

Blair RJ. Fine cuts of empathy and the amygdala: Dissociable deficits in psychopathy and autism. Q J Exp Psychol 2008; 61(1):157–170.

Blair T, Frith U. Neurocognitive explanations of the antisocial personality disorders. Crim Behav Ment Health 2000; 10(Suppl 1):S66–S81.

Blondel VD, Guillaume J-L, Lambiotte R, et al. Fast unfolding of communities in large networks. J Stat Mech Theory Exp 2008;2008(10):P10008.

Botvinick MM, Braver TS, Barch DM, et al. Conflict monitoring and cognitive control. Psychol Rev 2001;108(3):624–652; doi: 10.1037/0033-295x.108.3.624

Botvinick MM, Cohen JD, Carter CS. Conflict monitoring and anterior cingulate cortex: An update. Trends Cogn Sci 2004;8(12):539–546.

Botvinick MM. Conflict monitoring and decision making: Reconciling two perspectives on anterior cingulate function. Cogn Affect Behav Neurosci 2007;7(4):356–366.

Bush G, Luu P, Posner MI. Cognitive and emotional influences in anterior cingulate cortex. Trends Cogn Sci 2000;4(6):215–222.

Cameron JL. Interrelationships between hormones, behavior, and affect during adolescence: Understanding hormonal, physical, and brain changes occurring in association with pubertal activation of the reproductive axis. Introduction to part III. Ann N Y Acad Sci 2004;1021(1):110–123.

Celsis P, Boulanouar K, Doyon B, et al. Differential fMRI responses in the left posterior superior temporal gyrus and left supramarginal gyrus to habituation and change detection in syllables and tones. Neuroimage 1999;9(1):135–144.

Chang L. nltools: A suite of Python tools for conducting multivariate analysis of neuroimaging data; 2020. Available from: https://nltools.org/

Cohn MD, Veltman DJ, Pape LE, et al. Incentive processing in persistent disruptive behavior and psychopathic traits: A functional magnetic resonance imaging study in adolescents. Biol Psychiatry 2015;78(9):615–624; doi: 10.1016/j.biopsych.2014.08.017

Craig A. Emotional moments across time: A possible neural basis for time perception in the anterior insula. Philos Trans R Soc B Biol Sci 2009;364(1525):1933–1942.

Craig A. Significance of the insula for the evolution of human awareness of feelings from the body. Ann N Y Acad Sci 2011;1225(1):72–82.

Dahl RE. Adolescent brain development: A period of vulnerabilities and opportunities. Keynote address. Ann N Y Acad Sci 2004;1021(1):1–22.

Damoiseaux JS, Altmann A, Richiardi J, et al. Chapter 21—Applications of MRI Connectomics. In: Advances in Magnetic Resonance Technology and Applications, vol. 4. (Choi IY, Jezzard P. eds.) Academic Press; 2021; pp. 323–338.

De Vico Fallani F, Richiardi J, Chavez M, et al. Graph analysis of functional brain networks: Practical issues in translational neuroscience. Philos Trans R Soc Lond B Biol Sci 2014;369: 1653; doi: 10.1098/rstb.2013.0521

Deco G, Kringelbach ML. Great expectations: Using whole-brain computational connectomics for understanding neuropsychiatric disorders. Neuron 2014;84(5):892–905.

Desikan RS, Ségonne F, Fischl B, et al. An automated labeling system for subdividing the human cerebral cortex on MRI scans into gyral based regions of interest. Neuroimage 2006;31(3):968–980.

Dosenbach NU, Nardos B, Cohen AL, et al. Prediction of individual brain maturity using fMRI. Science 2010;329(5997): 1358–1361.

Dotterer HL, Hyde LW, Shaw DS, et al. Connections that characterize callousness: Affective features of psychopathy are associated with personalized patterns of resting-state network connectivity. Neuroimage Clin 2020;28:102402; doi: 10.1016/j.nicl.2020.102402

Dotterer HL, Hyde LW, Swartz JR, et al. Amygdala reactivity predicts adolescent antisocial behavior but not callous-unemotional traits. Dev Cogn Neurosci 2017;24:84–92.

Eckert MA, Menon V, Walczak A, et al. At the heart of the ventral attention system: The right anterior insula. Hum Brain Mapp 2009;30(8):2530–2541.

Fanti KA, Demetriou CA, Kimonis ER. Variants of callous-unemotional conduct problems in a community sample of adolescents. J Youth Adolesc 2013;42(7):964–979; doi: 10.1007/s10964-013-9958-9

Fanti KA, Kyranides MN, Petridou M, et al. Neurophysiological markers associated with heterogeneity in conduct problems, callous unemotional traits, and anxiety: Comparing children to young adults. Dev Psychol 2018;54(9):1634–1649; doi: 10.1037/dev0000505

Frick PJ, Ray JV, Thornton LC, et al. Annual research review: A developmental psychopathology approach to understanding callous-unemotional traits in children and adolescents with serious conduct problems. J Child Psychol Psychiatry 2014a;55(6):532–548.

Frick PJ, Ray JV, Thornton LC, et al. Can callous-unemotional traits enhance the understanding, diagnosis, and treatment of serious conduct problems in children and adolescents? A comprehensive review. Psychol Bull 2014b;140(1):1–57.

Frick PJ, White SF. Research review: The importance of callous-unemotional traits for developmental models of aggressive and antisocial behavior. J Child Psychol Psychiatry 2008; 49(4):359–375.

Frick PJ. The Inventory of Callous-Unemotional Traits. Unpublished Rating Scale. 2004.

Funayama ES, Grillon C, Davis M, et al. A double dissociation in the affective modulation of startle in humans: Effects of unilateral temporal lobectomy. J Cogn Neurosci 2001; 13(6):721–729.

Gates K. Homogeneity Assumptions in the Analysis of Dynamic Processes; 2022. Available from: https://osf.io/9zc8v

Gates KM, Molenaar PC. Group search algorithm recovers effective connectivity maps for individuals in homogeneous and heterogeneous samples. Neuroimage 2012;63(1):310–319.

Glasser MF, Sotiropoulos SN, Wilson JA, et al. The minimal preprocessing pipelines for the Human Connectome Project. Neuroimage 2013;80:105–124.

Gluckman NS, Hawes DJ, Russell AMT. Are callous-unemotional traits associated with conflict adaptation in childhood? Child Psychiatry Hum Dev 2016;47(4):583–592; doi: 10.1007/s10578-015-0593-4

Gratton C, Nomura EM, Pérez F, et al. Focal brain lesions to critical locations cause widespread disruption of the modular organization of the brain. J Cogn Neurosci 2012;24(6): 1275–1285; doi: 10.1162/jocn_a_00222

Guimera R, Nunes Amaral LA. Functional cartography of complex metabolic networks. Nature 2005;433(7028):895–900.

Hadjicharalambous MZ, Fanti KA. Self regulation, cognitive capacity and risk taking: Investigating heterogeneity among adolescents with callous-unemotional traits. Child Psychiatry Hum Dev 2018;49(3):331–340; doi: 10.1007/s10578-017-0753-9

Hadjikhani N, Joseph RM, Snyder J, et al. Anatomical differences in the mirror neuron system and social cognition network in autism. Cereb Cortex 2006;16(9):1276–1282.

Hamilton RB, Newman JP. The Response Modulation Hypothesis: Formulation, Development, and Implications for Psychopathy. In: Handbook of Psychopathy. (Patrick CJ. ed.) The Guilford Press, 2018; pp. 80–93.

Hamilton RK, Hiatt Racer K, Newman JP. Impaired integration in psychopathy: A unified theory of psychopathic dysfunction. Psychol Rev 2015;122(4):770.

Hawes DJ, Dadds MR. Revisiting the Role of Empathy in Childhood Pathways to Antisocial Behavior. In: Emotions, imagination, and moral reasoning. (Langdon R, Mackenzie C. eds.) Psychology Press, 2012; pp. 45–70.

He Y, Wang J, Wang L, et al. Uncovering intrinsic modular organization of spontaneous brain activity in humans. PLoS One 2009;4(4):e5226.

Honey CJ, Sporns O. Dynamical consequences of lesions in cortical networks. Hum Brain Mapp 2008;29(7):802–809; doi: 10.1002/hbm.20579

Jiang Y, Gao Y, Dong D, et al. Impaired global efficiency in boys with conduct disorder and high callous unemotional traits. J Psychiatr Res 2021;138:560–568.

Jones AP, Laurens KR, Herba CM, et al. Amygdala hypoactivity to fearful faces in boys with conduct problems and callous-unemotional traits. Am J Psychiatry 2009;166(1): 95–102.

Kahn RE, Byrd AL, Pardini DA. Callous-unemotional traits robustly predict future criminal offending in young men. Law Hum Behav 2013;37(2):87.

Kaiser RH, Andrews-Hanna JR, Wager TD, et al. Large-scale network dysfunction in major depressive disorder: A meta-analysis of resting-state functional connectivity. JAMA Psychiatry 2015;72(6):603–611.

Kiehl KA, Hoffman MB. The criminal psychopath: History, neuroscience, treatment, and economics. Jurimetrics 2011; 51:355–397.

Kimonis ER, Frick PJ, Skeem JL, et al. Assessing callous–unemotional traits in adolescent offenders: Validation of the Inventory of Callous–Unemotional Traits. Int J Law Psychiatry 2008;31(3):241–252.

Lancichinetti A, Fortunato S. Community detection algorithms: A comparative analysis. Phys Rev E 2009;80(5):056117.

Larson CL, Baskin-Sommers AR, Stout DM, et al. The interplay of attention and emotion: Top-down attention modulates amygdala activation in psychopathy. Cogn Affect Behav Neurosci 2013;13(4):757–770; doi: 10.3758/s13415-013-0172-8

Latora V, Marchiori M. Efficient behavior of small-world networks. Phys Rev Lett 2001;87(19):198701.

Leech R, Braga R, Sharp DJ. Echoes of the brain within the posterior cingulate cortex. J Neurosci 2012;32(1):215; doi: 10 .1523/jneurosci.3689-11.2012

Leech R, Sharp DJ. The role of the posterior cingulate cortex in cognition and disease. Brain 2014;137(1):12–32.

Leys C, Ley C, Klein O, et al. Detecting outliers: Do not use standard deviation around the mean, use absolute deviation around the median. J Exp Soc Psychol 2013;49(4):764–766.

Little TD, Bovaird JA, Widaman KF. On the merits of orthogonalizing powered and product terms: Implications for modeling interactions among latent variables. Struct Equ Modeling 2006;13(4):497–519; doi: 10.1207/s15328007sem1304_1

Marsh AA, Finger EC, Mitchell DG, et al. Reduced amygdala response to fearful expressions in children and adolescents with callous-unemotional traits and disruptive behavior disorders. Am J Psychiatry 2008;165(6):712–720.

Molenaar PCM. A manifesto on psychology as idiographic science: Bringing the person back into scientific psychology, this time forever. Measurement 2004;2(4):201–218; doi: 10 .1207/s15366359mea0204_1

Newman JP, Baskin-Sommers AR. Early selective attention abnormalities in psychopathy. Cogn Neurosci Attention 2012; 2021:421–440.

Newman ME, Girvan M. Finding and evaluating community structure in networks. Phys Rev E 2004;69(2):026113.

Nooner KB, Colcombe SJ, Tobe RH, et al. The NKI-Rockland sample: A model for accelerating the pace of discovery science in psychiatry. Front Neurosci 2012;6:152.

Park SH, Kim T, Ha M, et al. Intrinsic cerebellar functional connectivity of social cognition and theory of mind in first-episode psychosis patients. NPJ Schizophr 2021;7(1):59.

Patrick CJ. Emotion and psychopathy: Startling new insights. Psychophysiology 1994;31(4):319–330; doi: 10.1111/j .1469-8986.1994.tb02440.x

Pedregosa F, Varoquaux G, Gramfort A, et al. Scikit-learn: Machine learning in Python. J Mach Learn Res 2011;12: 2825–2830.

Penny WD, Friston KJ, Ashburner JT, et al. Statistical Parametric Mapping: The Analysis of Functional Brain Images. Elsevier; 2011.

Petersen AC, Crockett L, Richards M, et al. A self-report measure of pubertal status: Reliability, validity, and initial norms. J Youth Adolesc 1988;17(2):117–133.

Phelps EA, O'Connor KJ, Gatenby JC, et al. Activation of the left amygdala to a cognitive representation of fear. Nat Neurosci 2001;4(4):437–441.

Pu W, Luo Q, Jiang Y, et al. Alterations of brain functional architecture associated with psychopathic traits in male adolescents with conduct disorder. Sci Rep 2017;7(1):11349; doi: 10.1038/s41598-017-11775-z

Raschle NM, Menks WM, Fehlbaum LV, et al. Callous-unemotional traits and brain structure: Sex-specific effects in anterior insula of typically-developing youths. Neuroimage Clin 2018;17:856–864; doi: 10.1016/j.nicl.2017.12.015

Rubinov M, Sporns O. Complex network measures of brain connectivity: Uses and interpretations. Neuroimage 2010;52(3): 1059–1069; doi: 10.1016/j.neuroimage.2009.10.003

Rypma B, Prabhakaran V. When less is more and when more is more: The mediating roles of capacity and speed in brain-behavior efficiency. Intelligence 2009;37(2):207–222; doi: 10.1016/j.intell.2008.12.004

Seabold S, Perktold J. In: Proceedings of the 9th Python in Science Conference. Statsmodels: Econometric and statistical modeling with Python. 2010.

Seara-Cardoso A, Sebastian CL, Viding E, et al. Affective resonance in response to others' emotional faces varies with affective ratings and psychopathic traits in amygdala and anterior insula. Soc Neurosci 2016;11(2):140–152.

Seara-Cardoso A, Vasconcelos M, Sampaio A, et al. 3—Neural Correlates of Psychopathy: A Comprehensive Review. In: Psychopathy and Criminal Behavior. (Marques PB, Paulino M, Alho L. eds.) Academic Press; 2022; pp. 43–73.

Sebastian CL, McCrory EJP, Cecil CAM, et al. Neural responses to affective and cognitive theory of mind in children with conduct problems and varying levels of callous-unemotional traits. JAMA Psychiatry 2012;69(8):814–822.

Sisk CL, Foster DL. The neural basis of puberty and adolescence. Nat Neurosci 2004;7(10):1040–1047.

Smith SM, Miller KL, Salimi-Khorshidi G, et al. Network modelling methods for FMRI. Neuroimage 2011;54(2):875–891.

Sporns O, Honey CJ, Kötter R. Identification and classification of hubs in brain networks. PLoS One 2007;2(10):e1049.

Sun J, Bagrow JP, Bollt EM. et al. Dynamic computation of network statistics via updating schema. Phys Rev E 2009;79(3): 036116.

Tao Y, Rapp B. Investigating the network consequences of focal brain lesions through comparisons of real and simulated lesions. Sci Rep 2021;11(1):2213; doi: 10.1038/s41598-021-81107-9

Tosh CR, McNally L. The relative efficiency of modular and non-modular networks of different size. Proc R Soc B Biol Sci 2015;282(1802):20142568.

Touroutoglou A, Hollenbeck M, Dickerson BC, et al. Dissociable large-scale networks anchored in the right anterior insula subserve affective experience and attention. Neuroimage 2012;60(4):1947–1958.

Tzourio-Mazoyer N, Landeau B, Papathanassiou D, et al. Automated anatomical labeling of activations in SPM using a macroscopic anatomical parcellation of the MNI MRI single-subject brain. Neuroimage 2002;15(1):273–289.

Uddin LQ, Kelly AM, Biswal BB, et al. Functional connectivity of default mode network components: Correlation, anticorrelation, and causality. Hum Brain Mapp 2009;30(2):625–637; doi: 10.1002/hbm.20531

Umbach RH, Tottenham N. Callous-unemotional traits and reduced default mode network connectivity within a community sample of children. Dev Psychopathol 2021;33(4): 1170–1183.

Van Rossum G, Drake FL. Python 3 Reference Manual. CreateSpace: Scotts Valley, CA; 2009.

Varoquaux G, Gramfort A, Poline J-B, et al. Brain covariance selection: Better individual functional connectivity models using population prior. Adv Neural Inf Process Syst 2010; 2010:23.

Veroude K, von Rhein D, Chauvin RJ, et al. The link between callous-unemotional traits and neural mechanisms of reward processing: An fMRI study. Psychiatry Res Neuroimaging 2016;255:75–80.

Viding E, McCrory EJ. Genetic and neurocognitive contributions to the development of psychopathy. Dev Psychopathol 2012;24(3):969–983; doi: 10.1017/s095457941200048x

Viding E, Sebastian CL, Dadds MR, et al. Amygdala response to preattentive masked fear in children with conduct problems: The role of callous-unemotional traits. Am J Psychiatry 2012; 169(10):1109–1116.

Wechsler D. Wechsler Abbreviated Scale of Intelligence-(WASI-II), vol. 4. NCS Pearson; 2011.

White BA, Dede B, Heilman M, et al. Facial affect sensitivity training for young children with emerging CU traits: An experimental therapeutics approach. J Clin Child Adolesc Psychology 2022;51(3):264–276.

White SF, Brislin SJ, Meffert H, et al. Callous-unemotional traits modulate the neural response associated with punishing another individual during social exchange: A preliminary investigation. J Pers Disord 2013;27(1):99–112.

Whitfield-Gabrieli S, Nieto-Castanon A. Conn: A functional connectivity toolbox for correlated and anticorrelated brain networks. Brain Connect 2012;2(3):125–141; doi: 10.1089/brain.2012.0073

Winters DE, Brandon-Friedman R, Yepes G, et al. Systematic review and meta-analysis of socio-cognitive and socio-affective processes association with adolescent substance use. Drug Alcohol Depend 2021a;219:108479; doi: 10 .1016/j.drugalcdep.2020.108479

Winters DE, Hyde LW. Associated functional network connectivity between callous-unemotionality and cognitive and affective empathy. J Affect Disord 2022;318:304–313; doi: 10.1016/j.jad.2022.08.103

Winters DE, Leopold DR, Carter RM, et al. Resting-state connectivity underlying cognitive control's association with perspective taking in callous-unemotional traits. bioRxiv 2022; 2022:485718.

Winters DE, Pruitt PJ, Fukui S, et al. Network functional connectivity underlying dissociable cognitive and affective components of empathy in adolescence. Neuropsychologia 2021b; 156:107832; doi: 10.1016/j.neuropsychologia.2021.107832

Winters DE, Sakai JT, Carter RM. Resting-state network topology characterizing callous-unemotional traits in adolescence. Neuroimage Clin 2021c;32:102878; doi: 10.1016/j.nicl.2021 .102878

Winters DE, Sakai JT. Affective theory of mind impairments underlying callous-unemotional traits and the role of cognitive control: A pilot study. PsyArXiv 2021;2021:8; doi: 10 .31234/osf.io/stwj8

Winters DE. resmod: A package for creating orthogonalized interaction terms by centering residuals; 2022. Available from: https://pypi.org/project/resmod/

Wu CW, Chen C-L, Liu P-Y, et al. Empirical evaluations of slice-timing, smoothing, and normalization effects in seed-based, resting-state functional magnetic resonance imaging analyses. Brain Connect 2011;1(5):401–410.

Yang Y, Raine A, Narr KL, et al. Localization of deformations within the amygdala in individuals with psychopathy. Arch Gen Psychiatry 2009;66(9):986–994.

Yarkoni T, Poldrack RA, Nichols TE, et al. Large-scale automated synthesis of human functional neuroimaging data. Nat Methods 2011;8(8):665–670; doi: 10.1038/nmeth.1635

Yoder KJ, Lahey BB, Decety J. Callous traits in children with and without conduct problems predict reduced connectivity when viewing harm to others. Sci Rep 2016;6(1):20216; doi: 10.1038/srep20216

Address correspondence to:
Drew E. Winters
Department of Psychiatry
University of Colorado School of Medicine Anschutz Medical Campus
1300 East 17th Place
Aurora, CO 80045-2559
USA

E-mail: drew.winters@cuanschutz.edu